Magnesium-Containing Polyanion and Intermediate Europium Valence: Crystal Structure, Chemical Bonding, and Properties of $EuMg_{1-x}Tl_{1+x}$ ($x = 0.013-0.058$)

Rainer Kraft,[†] Rolf-Dieter Hoffmann,[†] C. Peter Sebastian,[†] Rainer Pöttgen,*[,†] Yurii Prots,[‡] Walter Schnelle,[‡] Marcus Schmidt,[‡] and Yuri Grin[‡]

Institut für Anorganische und Analytische Chemie and NRW Graduate School of Chemistry, Universität Münster, Corrensstrasse 36, 48149 Münster, Germany, and Max-Planck-Institut für Chemische Physik fester Stoffe, Nöthnitzer Strasse 40, 01187 Dresden, Germany

Received May 16, 2007. Revised Manuscript Received December 4, 2007

The ternary europium−magnesium−thallium phase $EuMg_{1-x}Tl_{1+x}$ ($x = 0.013$–0.058) was synthesized from the elements by induction melting in sealed tantalum tubes in a water-cooled quartz sample chamber. The new phase crystallizes with the orthorhombic TiNiSi type of structure (space group *Pnma*, $Z = 4$). The crystal structures were investigated using powder and single-crystal X-ray diffraction, which gave the following results (21 variables per refinement): $a = 805.3(1)$ pm, $b = 493.5(1)$ pm, $c = 874.6(1)$ pm, and $wR2 = 0.058$, based on 673 F^2 values for $EuMg_{0.942(4)}Tl_{1.058(4)}$; $a = 806.2(1)$ pm, $b = 493.39(8)$ pm, $c = 873.9(1)$ pm, and $wR2 = 0.047$, based on 814 F^2 values for $EuMg_{0.987(2)}Tl_{1.013(2)}$; and $a = 806.6(2)$ pm, $b = 493.65(8)$ pm, $c = 874.0(1)$ pm, and $wR2 = 0.033$, based on 675 F^2 values for $EuMg_{0.983(2)}Tl_{1.017(2)}$. All of the crystals revealed a small amount of Mg/Tl mixing on the magnesium site. Chemical bonding analysis using an electron localization function approach revealed a three-dimensional, covalently bonded $[Mg_{1-x}Tl_{1+x}]$ network in which the europium atoms fill slightly distorted hexagonal prismatic channels. Temperature-dependent magnetization measurements of a EuMgTl sample out of the homogeneity range detected Curie−Weiss paramagnetism above 100 K with an effective magnetic moment of 7.84(5) μ_B/Eu atom. EuMgTl ordered ferromagnetically at 23.1(5) K. ^{151}Eu Mössbauer spectroscopy measurements showed two signals at 78 K [$\delta = -10.14(1)$ and 0.62(5) mm/s, corresponding to Eu^{2+} and Eu^{3+}, respectively] in a ratio of 86/14, indicating the presence of a significant amount of trivalent europium in EuMgTl. At 4.2 K, full magnetic hyperfine field splitting with a hyperfine field of 23.4(4) T was observed for divalent europium. The partial oxidation of europium to the trivalent state was corroborated by Eu L_{III} X-ray absorption spectroscopy data.

1. Introduction

The equiatomic Eu*TX* intermetallic compounds (T = a late transition element; X = an element of the third, fourth, or fifth main group) have been investigated intensively during the last twenty years with respect to their crystal chemistries and greatly varying physical properties. At present, more than 70 Eu*TX* compounds are known and have been found to crystallize in 12 different structure types. The transition-metal and main-group-element atoms build up two- or three-dimensional [*TX*] networks, within which the europium atoms fill cages or channels. The structure−property relations of these peculiar materials have been summarized in a recent review article.[1] In most Eu*TX* compounds, the europium atoms have a stable $4f^7$ configuration, and magnetic susceptibility measurements have revealed ferromagnetic ordering of the europium magnetic moments at low temperatures. The magnetic hyperfine field splitting could be monitored effectively using temperature-dependent ^{151}Eu Mössbauer spectroscopic data.

Recent investigations have revealed that the main-group elements in the various Eu*TX* compounds can be completely substituted with magnesium or cadmium. Cell volumes and magnetic susceptibility data indicated the presence of divalent europium for both EuMg*T* (T = Ag, Au) and EuCd*T* (T = Pd, Ag, Au).[2–6] This is a very interesting situation from the point of view of chemical bonding, since at least magnesium is clearly more electropositive than the transition metals.

In further studies on similar equiatomic rare-earth compounds, it was also possible to substitute the transition metal by an element of the third main group, leading to the series of compounds *RE*MgGa, *RE*MgIn, and *RE*MgTl (*RE* = rare-earth element).[7–11] These gallides, indides, and thallides are interesting from the point of view of their physical properties.

* To whom correspondence should be addressed. E-mail: pottgen@uni-muenster.de.
[†] Universität Münster.
[‡] Max-Planck-Institut für Chemische Physik fester Stoffe.

(1) Pöttgen, R.; Johrendt, D. *Chem. Mater.* **2000**, *12*, 875.
(2) Mishra, R.; Pöttgen, R.; Hoffmann, R.-D.; Kaczorowski, D.; Piotrowski, H.; Mayer, P.; Rosenhahn, C.; Mosel, B. D. *Z. Anorg. Allg. Chem.* **2001**, *627*, 1283.
(3) Fickenscher, T.; Kotzyba, G.; Hoffmann, R.-D.; Pöttgen, R. *Z. Naturforsch.* **2001**, *56b*, 598.
(4) Fickenscher, T.; Pöttgen, R. *J. Solid State Chem.* **2001**, *161*, 67.
(5) Fickenscher, T.; Hoffmann, R.-D.; Mishra, R.; Pöttgen, R. *Z. Naturforsch.* **2002**, *57b*, 275.
(6) Johrendt, D.; Kotzyba, G.; Trill, H.; Mosel, B. D.; Eckert, H.; Fickenscher, T.; Pöttgen, R. *J. Solid State Chem.* **2002**, *164*, 201.
(7) Canepa, F.; Fornasini, M. L.; Merlo, F.; Napoletano, M.; Pani, M. *J. Alloys Compd.* **2000**, *312*, 12.
(8) Kraft, R.; Valldor, M.; Pöttgen, R. *Z. Naturforsch.* **2003**, *58b*, 827.

10.1021/cm071325i CCC: $40.75
Published on Web 01/19/2008

*RE*MgGa, *RE*MgIn, and *RE*MgTl compounds containing trivalent rare-earth metals crystallize with the hexagonal ZrNiAl type structure,[12–14] as do many *RETX* intermetallics.[15,16] Also, the magnetic behavior of the rare-earth component of the *RE*Mg*X* compounds does not depend on 4f−3d hybridization, and one can expect different magnetic coupling.

To date, only the metamagnet CeMgGa (T_N = 3.1 K),[17] antiferromagnetic GdMgGa (T_N = 15.3 K), paramagnetic GdMgIn,[7] and the antiferromagnets DyMgIn (T_N = 22 K), HoMgIn (T_N = 12 K), and TmMgIn (T_N = 3 K) have been studied with respect to their magnetic properties.[9] Here we report on the synthesis, structure, chemical bonding, and physical properties of the new phase $EuMg_{1-x}Tl_{1+x}$ (x = 0.013–0.058), which shows a narrow homogeneity range.

2. Experimental Procedures

2.1. Syntheses. Starting materials for the syntheses of the $EuMg_{1-x}Tl_{1+x}$ samples (x = −0.10, ±0.05, ±0.025, 0) were sublimed ingots of europium (Johnson Matthey, >99.9%), a magnesium rod (Johnson Matthey, 16 mm diameter, >99.5%), and thallium granules (Chempur, 1–5 mm diameter, >99.999%, kept under water). The air- and moisture-sensitive europium ingots were kept in Schlenk tubes under dry argon prior to the reactions. Argon was purified over a titanium sponge (900 K), silica gel, and molecular sieves. Pieces of europium, portions of the magnesium rod (after cutting the surface of the rod on a turning lathe in order to remove surface impurities), and thallium granules (after drying) were weighed in the ratios listed above and sealed in tantalum ampoules under an argon pressure of 800 mbar in an arc-melting apparatus.[18]

The tantalum ampoules were subsequently placed in the water-cooled sample chamber of an induction furnace[19] (Hüttinger Elektronik, Freiburg, Germany, Typ TIG 2.5/300), heated to 1500 K, and kept at that temperature for 10 min. Finally, the temperature was lowered to 900 K, and the samples were annealed at that temperature for another 4 h and then cooled within the furnace after the power was switched off. The temperature was controlled using a Sensor Therm Metis MS09 pyrometer with an accuracy of ±20 K. The brittle products could easily be separated from the tantalum tubes. No reaction with the container material was observed. The compact light-gray pieces and the dark-gray powder were stable in air for some time. However, the samples were kept in argon-filled Schlenk tubes in order to prevent hydrolysis by atmospheric moisture. The single crystals investigated on the diffractometers and the bulk samples were analyzed using a Leica 420 I scanning electron microscope. No impurity elements were detected.

Caution: Thallium metal and its salts are toxic. Extreme care must be employed in handling these materials and in disposing of their wastes.

Table 1. Lattice Parameters of $EuMg_{1-x}Tl_{1+x}$ (x = −0.05 to 0.1)

sample (starting composition)	a (pm)	b (pm)	c (pm)	V (nm^3)
$EuMg_{0.9}Tl_{1.1}$	804.6(1)	494.53(9)	875.2(1)	0.3482
$EuMg_{0.942}Tl_{1.058}$[a]	804.4(2)	492.8(1)	872.9(2)	0.3460
$EuMg_{0.95}Tl_{1.05}$	805.3(1)	493.5(1)	874.6(1)	0.3475
$EuMg_{0.975}Tl_{1.025}$	806.2(1)	493.39(8)	873.9(1)	0.3476
$EuMg_{0.987}Tl_{1.013}$[a]	805.3(2)	492.5(1)	873.5(2)	0.3464
$EuMg_{0.983}Tl_{1.017}$[a]	805.3(2)	492.3(1)	873.3(2)	0.3462
EuMgTl	806.6(2)	493.65(8)	874.0(1)	0.3480
$EuMg_{1.025}Tl_{0.975}$	805.9(1)	493.68(7)	874.2(1)	0.3478
$EuMg_{1.05}Tl_{0.95}$	806.9(1)	493.51(5)	874.72(9)	0.3483

[a] Single-crystal data.

2.2. X-ray Diffraction Investigations. The samples were characterized through Guinier powder patterns using Cu Kα_1 radiation (λ = 154.06 pm) and α-quartz (a = 491.30 pm, c = 540.46 pm) as an internal standard. The Guinier camera was equipped with an imaging plate detector (Fujifilm BAS-1800). To ensure correct indexing, the observed patterns were compared with calculated ones[20] taking the positions of the refined structures. The refined lattice parameters are listed in Table 1. The lattice parameters obtained from the single-crystal diffractometer and those refined from the powders (Table 1) were in good agreement.

Small, irregularly shaped single crystals were isolated from the annealed $EuMg_{1-x}Tl_{1+x}$ specimens by mechanical fragmentation. They were investigated on a Buerger precession camera equipped with an imaging plate system (Fujifilm BAS-1800) in order to establish both symmetry and suitability for collection of intensity data.

Intensity data for suitable single crystals were recorded at room temperature using a STOE imaging plate system (IPDS-II) with graphite-monochromatized Mo Kα or Ag Kα radiation in oscillation mode. Numerical absorption corrections were applied to these data. All relevant crystallographic data and details concerning collection and evaluation of the data are listed in Table 2.

Analysis of the diffraction data revealed that all of the samples crystallize with the orthorhombic TiNiSi type of structure[21] (space group *Pnma*). The starting atomic positions were deduced by direct methods with SHELXS-97.[22] The structures were then refined with SHELXL-97[23] using anisotropic displacement parameters for all sites. As a check for the correct composition, the occupancy parameters of all sites were refined in separate series of least-squares cycles. While the europium and thallium positions were fully occupied within one standard deviation, the magnesium sites of all of the crystals revealed a higher scattering power. This indicated Mg/Tl mixing for this position. In the following cycles, the structures were refined using the mixed Mg/Tl occupancy as a least-squares variable, leading to the compositions listed in Table 2. Subsequent difference Fourier syntheses revealed no significant residual peaks. The refined positional parameters are listed in Table 3. As an example, we list the interatomic distances of $EuMg_{0.983}Tl_{1.017}$ (along with those of isopointal EuMgPd for

(9) Kraft, R.; Valldor, M.; Kurowski, D.; Hoffmann, R.-D.; Pöttgen, R. *Z. Naturforsch.* **2004**, *59b*, 513.
(10) Kraft, R.; Pöttgen, R. *Z. Naturforsch.* **2005**, *60b*, 265.
(11) Fedorchuk, A.; Prots, Y.; Schnelle, W.; Schmidt, M.; Grin, Y. *Z. Kristallogr.* **2005**, Suppl. 22, 177.
(12) Krypyakevich, P. I.; Markiv, V. Y.; Melnyk, E. V. *Dopov. Akad. Nauk Ukr. RSR, Ser. A* **1967**, 750.
(13) Dwight, A. E.; Mueller, M. H.; Conner, R. A., Jr.; Downey, J. W.; Knott, H. *Trans. Metall. Soc. AIME* **1968**, *242*, 2075.
(14) Zumdick, M. F.; Hoffmann, R.-D.; Pöttgen, R. *Z. Naturforsch.* **1999**, *54b*, 45.
(15) Villars, P.; Calvert, L. D. *Pearson's Handbook of Crystallographic Data for Intermetallic Compounds*, 2nd and desk eds.; American Society for Metals: Materials Park, OH, 1991 and 1997.
(16) Szytuła, A.; Leciejewicz, J. *Handbook of Crystal Structures and Magnetic Properties of Rare Earth Intermetallics*; CRC Press: Boca Raton, FL, 1994.
(17) Kraft, R.; Pöttgen, R.; Kaczorowski, D. *Chem. Mater.* **2003**, *15*, 2998.
(18) Pöttgen, R.; Gulden, T.; Simon, A. *GIT Labor-Fachz.* **1999**, *43*, 133.
(19) Kussmann, D.; Hoffmann, R.-D.; Pöttgen, R. *Z. Anorg. Allg. Chem.* **1998**, *624*, 1727.
(20) Yvon, K.; Jeitschko, W.; Parthé, E. *J. Appl. Crystallogr.* **1977**, *10*, 73.
(21) Shoemaker, C. B.; Shoemaker, D. P. *Acta Crystallogr.* **1965**, *18*, 900.
(22) Sheldrick, G. M. *SHELXS-97, Program for Crystal Structure Refinement*; University of Göttingen: Göttingen, Germany, 1997.
(23) Sheldrick, G. M. *SHELXL-97, Program for Determination of Crystal Structures*; University of Göttingen: Göttingen, Germany, 1997.

Table 2. Crystallographic Data for $EuMg_{1-x}Tl_{1+x}$ (TiNiSi Type of Structure, Space Group *Pnma*, $Z = 4$)

	$EuMg_{0.95}Tl_{1.05}$	$EuMg_{0.975}Tl_{1.025}$	EuMgTl
refined composition	$EuMg_{0.942(4)}Tl_{1.058(4)}$	$EuMg_{0.987(2)}Tl_{1.013(2)}$	$EuMg_{0.983(2)}Tl_{1.017(2)}$
wavelength, λ (nm)	0.56087	0.71073	0.56087
molar mass (g/mol)	391.10	382.99	383.71
unit-cell dimensions	Table 1	Table 1	Table 1
calculated density (g/cm^3)	7.47	7.32	7.33
crystal dimensions (μm $\times$ μm $\times$ μm)	30 $\times$ 40 $\times$ 60	30 $\times$ 40 $\times$ 100	40 $\times$ 60 $\times$ 100
transm. ratio (max/min)	2.45	2.56	1.38
absorption coefficient (mm^{-1})	36.2	64.6	35.1
F(000)	640	627	629
θ range for data collection (deg)	2−26	3−35	2−26
ranges for h, k, l	$\pm$12, $\pm$7, $\pm$13	$\pm$12, $\pm$7, $-14 \le l \le 12$	$\pm$12, $\pm$7, $\pm$13
total no. of reflections	5909	4330	5934
no. of independent reflections	673 ($R_{int} = 0.108$)	814 ($R_{int} = 0.035$)	675 ($R_{int} = 0.044$)
no. of reflections for which $I > 2\sigma(I)$	568 ($R_{sigma} = 0.045$)	777 ($R_{sigma} = 0.020$)	600 ($R_{sigma} = 0.021$)
no. of data points/parameters	673/21	814/21	675/21
goodness-of-fit on F^2	1.067	1.180	1.046
final $R1$, $wR2$ indices [$I > 2\sigma(I)$]	0.030, 0.055	0.024, 0.047	0.020, 0.032
$R1$, $wR2$ indices (all data)	0.042, 0.058	0.026, 0.047	0.027, 0.033
extinction coefficient	0.0010(3)	0.0063(4)	0.0013(2)
largest diff. peak and hole (e/Å^3)	2.36 and −2.12	1.95 and −1.72	1.22 and −1.64

Table 3. Positional Parameters and Isotropic Displacement Parameters (pm^2) in the Solid Solution $EuMg_{1-x}Tl_{1+x}$[a]

site	occupancy[b]	x	y	z	U_{eq}[c]
		$EuMg_{0.942(4)}Tl_{1.058(4)}$			
Eu	1.00	0.00838(6)	1/4	0.69202(6)	125(1)
Mg	0.942(4)	0.1658(4)	1/4	0.0708(3)	161(10)
Tl	1.00	0.28322(5)	1/4	0.39328(5)	130(1)
		$EuMg_{0.987(2)}Tl_{1.013(2)}$			
Eu	1.00	0.00879(4)	1/4	0.69068(4)	165(1)
Mg	0.987(2)	0.1609(3)	1/4	0.0694(3)	188(9)
Tl	1.00	0.28321(3)	1/4	0.39223(3)	169(1)
		$EuMg_{0.983(2)}Tl_{1.017(2)}$			
Eu	1.00	0.00875(5)	1/4	0.69058(4)	129(1)
Mg	0.983(2)	0.1606(4)	1/4	0.0689(3)	169(10)
Tl	1.00	0.28337(4)	1/4	0.39210(3)	132(1)

[a] All atoms occupy Wyckoff position 4*c* of space group *Pnma*. [b] Values less than 1.00 for Mg sites indicate Mg/Tl mixing; the value given is the fraction of sites occupied by Mg. [c] U_{eq} is defined as one-third of the trace of the orthogonalized U_{ij} tensor.

comparison) in Table 4. Further details concerning the structure refinements are available.[24]

The EuMgTl sample (1/1/1 starting composition) was also investigated using a STOE STADI P powder diffractometer with Cu Kα_1 radiation in order to perform a full-profile Rietveld refinement. The data are presented in Figure 1. The measurement was performed in transmission geometry using Cu Kα_1 radiation ($\lambda = 154.0598$ pm, Ge monochromator). The Rietveld calculations were performed using the FullProf_2k software.[25] The background was set manually, and the profiles were modeled using the pseudo-Voigt function. The results of the refinement are summarized in Table 5. The powder data fully confirmed the structure of EuMgTl, and we were able to show that the sample contained only one phase at the detection level of the X-ray powder diffraction experiment.

2.3. Magnetism, ^{151}Eu Mössbauer Spectroscopy, and XAS Measurements. Magnetization measurements were carried out using a Physical Property Measurement System (Quantum Design) over the temperature range 4.2−300 K with magnetic flux densities up to 8 T.

Table 4. Interatomic Distances (pm) in the Coordination Spheres of Atoms in the Crystal Structures of $EuMg_{0.983}Tl_{1.017}$ and EuPdMg[a]

	$EuMg_{0.983}Tl_{1.017}$				EuPdMg[b]		
Eu:	1	Tl	342.4(1)	Eu:	2	Pd	317.0(1)
	2	Tl	346.5(1)		1	Pd	318.1(2)
	2	Tl	348.7(1)		2	Pd	321.7(1)
	2	Mg	351.6(2)		2	Mg	339.4(5)
	1	Mg	352.7(2)		1	Mg	343.3(7)
	1	Mg	360.9(2)		2	Mg	348.6(6)
	2	Mg	378.6(2)		1	Mg	361.6(7)
	1	Tl	407.5(1)		2	Eu	380.3(2)
	2	Eu	414.9(1)		2	Eu	397.5(1)
Tl:	2	Mg	294.7(1)	Pd:	1	Mg	277.7(8)
	1	Mg	299.3(2)		2	Mg	279.9(4)
	1	Mg	306.2(3)		1	Mg	292.8(7)
	1	Eu	342.4(1)		2	Eu	317.0(1)
	2	Eu	346.5(1)		1	Eu	318.1(2)
	2	Eu	348.7(1)		2	Eu	321.7(1)
Mg:	2	Tl	294.7(1)	Mg:	1	Pd	277.7(8)
	1	Tl	299.3(2)		2	Pd	279.9(4)
	1	Tl	306.2(3)		1	Pd	292.8(7)
	2	Eu	351.6(2)		2	Mg	320.4(8)
	1	Eu	352.7(2)		2	Eu	339.4(5)
	1	Eu	360.9(2)		1	Eu	343.3(7)
	2	Mg	377.7(4)		2	Eu	348.6(6)
	1	Mg	378.6(2)		1	Eu	361.7(7)

[a] Standard deviations are given in parentheses. Note that the magnesium position shows a small Mg/Tl mixed occupancy (see Table 3). [b] Data taken from ref 28.

The 21.53 keV transition of ^{151}Eu with an activity of 130 MBq (2% of the total activity of a ^{151}Sm:EuF_3 source) was used for Mössbauer spectroscopy experiments. The temperature of the absorber was varied between 4.2 and 78 K, while the source was kept at room temperature. The sample was placed within a thin-walled PVC container at a thickness corresponding to 10 mg of Eu/cm^2.

Eu L_{III} X-ray absorption spectra (XAS) of polycrystalline EuMgTl were recorded in transmission geometry at the EXAFS II beamline E4 of HASYLAB at DESY. Wavelength selection was realized using a Si(111) double-crystal monochromator that yielded a resolution of 2 eV (fwhm) for the chosen setup at the Eu L_{III} threshold of 6977 eV. Experimental data were measured using EuF_3 as an external reference for energy calibration. Deconvolution of the XAS spectra was performed using the program XASWin.[26]

(24) Details may be obtained from Fachinformationszentrum Karlsruhe, D-76344 Eggenstein-Leopoldshafen, Germany (e-mail: crysdata@fiz-karlsruhe.de), by quoting Registry Nos. CSD-416496 ($EuMg_{0.942}Tl_{1.058}$), CSD-416497 ($EuMg_{0.987}Tl_{1.013}$), and CSD-416495 ($EuMg_{0.983}Tl_{1.017}$).

(25) Roisnel, T.; Rodríguez-Carvajal, J. *FullProf_2k*, version 2.0; Laboratoire Léon Brillouin (CEA-CNRS): Gif-sur-Yvette, France, 2001.

(26) Akselrud, L.; Grin, Y. *XASWin Program*; Max-Planck-Institut für Chemische Physik fester Stoffe: Dresden, Germany, 2004.

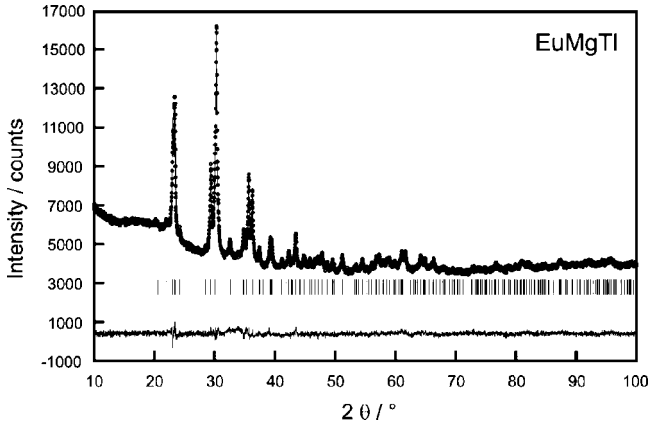

Figure 1. (top) Experimentally observed (solid circles) and calculated (solid line) X-ray powder diffraction patterns for EuMgTl. (middle) Vertical lines indicating the Bragg reflection positions. (bottom) The intensity difference I(obs) − I(calc).

Table 5. X-ray Powder Diffraction Data and Structure Refinement for EuMgTl

composition	EuMgTl
formula mass (g/mol)	380.64
lattice parameters	Table 1
unit-cell volume (nm^3)	0.3450
calculated density (g/cm^3)	7.27
absorption correction (μR)	1.40
F(000)	624
2θ range (deg)	5–100
scan mode, step width (deg 2θ)	$\theta/2\theta$, 0.03
no. of data points	4751
no. of Bragg reflections	230
asymmetry parameters	0.016(2), −0.0019(4)
no. of structure parameters	13
total no. of refined parameters	21
R_F, R_{wp}	0.088, 0.134
$R_{Bragg}(I)$	0.078
χ^2	1.76
Bérar−Lelann factor	3.50

2.4. Quantum-Chemical Calculations. Electronic structure calculations and bonding analyses using the TB-LMTO-ASA program package[27] were performed on EuMgPd[28] and the ordered EuMgTl model without taking into account the mixed occupation of the magnesium position. The Barth−Hedin exchange potential[29] was employed for local density approximation calculations. The radial scalar-relativistic Dirac equation was solved to obtain the partial waves. Although calculations within the atomic sphere approximation (ASA) include corrections for the neglect of interstitial regions and partial waves of higher order,[30] addition of empty spheres was not necessary for either compound. The following atomic-sphere radii were applied in the EuMgTl calculations: r(Eu) = 2.199 Å, r(Mg) = 1.643 Å, and r(Tl) = 1.791 Å. In the EuMgPd calculations, the following radii were used: r(Eu) = 2.074 Å, r(Mg) = 1.622 Å, and r(Pd) = 1.583 Å. Basis sets containing Eu(6s, 5d, 4f), Mg(3s, 3p), and Tl(6s, 6p) or Pd(5s, 5p, 4d) orbitals were employed for self-consistent field calculations, with the Eu(6p), Mg(3d), and Tl(5d) or Pd(4f) functions being downfolded. Spin-polarized calculations were performed.

The electron localization function (ELF) was evaluated according to ref 31 using the ELF module implemented within the TB-LMTO-ASA program package.[27] The topology of the ELF was analyzed using the program Basin,[32] which performs consecutive integration of the electron density in basins that are bounded by zero-flux surfaces in the ELF gradient field. This procedure (the ELF/electron density approach), which is similar to the one proposed by Bader for the electron density,[33] allows the assignment of an electron count for each basin, thereby revealing basic information about the chemical bonding.

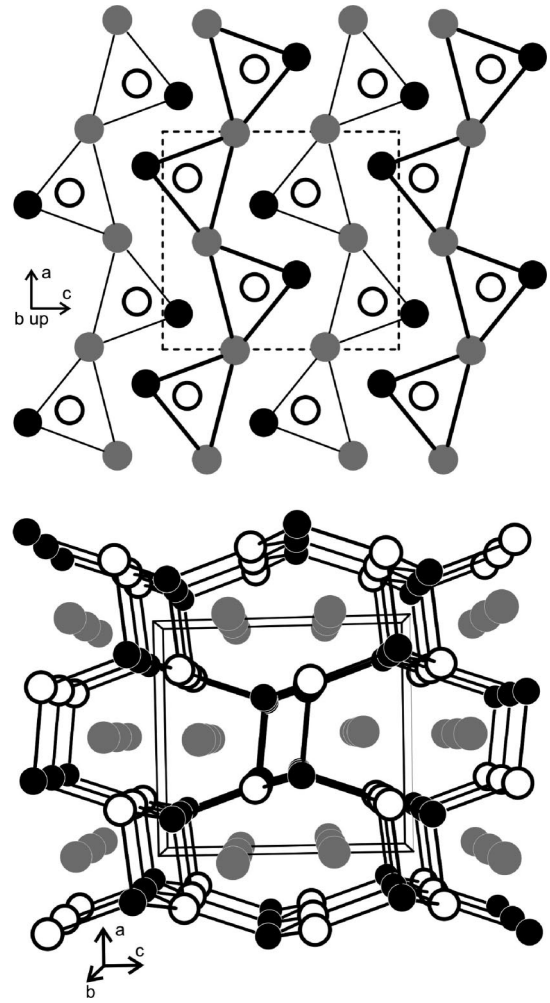

Figure 2. Crystal structure of EuMgTl. Europium, magnesium, and thallium atoms are drawn as solid gray, solid black, and open circles, respectively. The magnesium site shows a small mixed occupancy with thallium (Table 3). (top) Projection of the structure onto the *ac* plane. All atoms lie on mirror planes at $y = {}^1/_4$ (thin lines) and $y = {}^3/_4$ (thick lines). The trigonal prismatic coordination of thallium is emphasized. (bottom) Three-dimensional [MgTl] network.

3. Results and Discussion

3.1. Crystal Chemistry. The structure of EuMgTl is presented in Figure 2. For clarity, here we refer only to the stoichiometric composition assuming full occupancy of the Mg site by magnesium. The small homogeneity range is discussed in detail in the chemical bonding discussion below. EuMgTl crystallizes with the orthorhombic TiNiSi type of structure[21] (space group *Pnma*). This structure type can be

(27) Jepsen, O.; Burkhardt, A.; Andersen, O. K. *The TB-LMTO-ASA Program*, version 4.7; Max-Planck-Institut für Festkörperforschung: Stuttgart, Germany, 1999.
(28) Kraft, R.; Fickenscher, T.; Kotzyba, G.; Hoffmann, R.-D.; Pöttgen, R. *Intermetallics* **2003**, *11*, 111.
(29) Barth, U.; Hedin, L. *J. Phys. C* **1972**, *5*, 1629.
(30) Andersen, O. K. *Phys. Rev. B* **1975**, *12*, 3060.
(32) Kohout, M. *Basin*, version 4.1; Max-Planck-Institut für Chemische Physik fester Stoffe: Dresden, Germany, 2006.
(33) Bader, R. F. W. *Atoms in Molecules: A Quantum Theory*; Oxford University Press: Oxford, U.K., 1999.

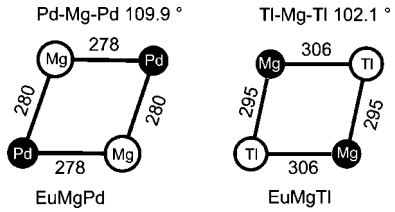

Figure 3. Comparison of interatomic distances (pm) and bond angles (deg) in the Mg_2Pd_2 and Mg_2Tl_2 units found in the crystal structures of EuMgPd and EuMgTl, respectively (see text for details).

considered as a ternary-ordered version of the binary KHg_2 type[34,35] (space group *Imma*) obtained through a *klassengleiche* symmetry reduction. The binary phases $EuTl_2$[36] and $EuMg_2$,[37] however, crystallize with the $CaIn_2$[36] and $MgZn_2$ types,[38,39] respectively.

From a geometrical point of view, the EuMgTl structure can be constructed from thallium-centered Eu_4Mg_2 trigonal prisms (Figure 2). These prisms are condensed via common edges in the *a* direction, forming chains that are situated at two different heights and separated by half of the translation period *b*. In the latter direction, the prisms are condensed via common triangular faces.

The shortest distances (295−306 pm) in the EuMgTl structure occur for Mg−Tl contacts. These Mg−Tl distances are slightly longer than the sum of the covalent radii (291 pm) but clearly smaller than the sum of metallic radii (330 pm);[40] they are similar to those in the series of *RE*MgTl compounds[10] having the hexagonal ZrNiAl type structure (i.e., 299 and 303 pm in CeMgTl[10]). These findings suggest the formation of a three-dimensional [MgTl] network (Figure 2), which is rather unexpected considering the large difference in electronegativity between magnesium and thallium.

The three-dimensional [MgTl] network contains slightly distorted hexagonal prismatic channels that are filled by the europium atoms. Despite the larger covalent radius of thallium (155 pm) compared with magnesium (136 pm),[40] the shortest contacts of the europium atoms with the network are those of Eu−Tl, which range from 342 to 349 pm.

At this point it is worthwhile to compare the structure of EuMgTl with that of EuMgPd.[28] Both structures are isotypic. As emphasized in Figure 3, the Mg_2Pd_2 and Mg_2Tl_2 parallelograms in EuMgPd and EuMgTl, respectively, are both right-tilted, leading to a maximal separation of the more-electronegative palladium and thallium atoms. Given the large difference in the electronegativities of europium or magnesium on one hand and palladium or thallium on the other (the Pauling electronegativities of Mg, Pd, and Tl are 1.31, 2.20, and 2.04, respectively[40]), EuMgPd should be considered as a palladide and EuMgTl as a thallide. An interesting difference in the two structures concerns the Mg−Mg distances. Only in EuMgPd, which contains the smaller palladium atoms, does one observe a short Mg−Mg contact of 320 pm (Table 4) similar to the average Mg−Mg distance of 320 pm found in hcp magnesium.[41]

For the discussion of chemical bonding in $EuMg_{1-x}Tl_{1+x}$, we start with the Zintl phase $EuTl_2$ ($CaIn_2$ type).[36] The crystal structure contains interconnected puckered nets formed by quadruply bonded thallium atoms. According to the Zintl rule, the europium atoms transfer two valence electrons each to the thallium atoms, and the Tl^- anions build up a lonsdaleite-related tetrahedral network of quadruply bonded atoms. This model was confirmed through ELF bonding analysis of another chemical analogue of EuMgTl, namely, $EuGa_2$,[42] which crystallizes in the orthorhombic KHg_2 type of structure mentioned above. The europium atoms are embedded in the three-dimensional framework formed by quadruply bonded gallium atoms, which is very similar to the [MgTl] framework in EuMgTl. ELF analysis confirmed the covalent bonding within the gallium framework. On the basis of the ELF/electron density approach, $EuGa_2$ was described as an electron-balanced compound: each Eu^{2+} ion is balanced by two Ga^- ions. Despite the similar crystal structures, direct transfer of this bonding scheme from $EuTl_2$ or $EuGa_2$ to EuMgTl would give a structure that is not electron-balanced: each Eu^{2+} ion would be matched with a $[MgTl]^{3-}$ ion. This suggests that either the europium exists as Eu^{3+} or a different bonding model for the polyanion applies. To shed more light on the bonding situation in EuMgTl, we performed quantum-chemical calculations.

The topology of the ELF in EuMgTl is very similar to that in $EuGa_2$. The maxima of the ELF (attractors) are located close to the short Mg−Tl contacts (Figure 4a), indicating the covalent interaction within the [MgTl] network. No additional attractors were found between the europium atoms and the atoms of the network, suggesting an ionic interaction in this part of the crystal structure. Whereas the inner shells of magnesium and thallium possess spherical shapes, the fifth shell of europium is structured (i.e., it deviates from spherical shape, Figure 4b), which suggests that some of these electrons participate in the valence interactions (i.e., that the oxidation state of europium is higher than 2+).[43] In addition, the electronic density of states (DOS) for EuMgTl (Figure 5) reveals a pseudogap behavior, especially when the Eu(4f) contributions are excluded. All of these findings suggest that the Mg/Tl polyanion is electron-deficient, assuming ideal equiatomic composition and the Eu^{2+} configuration. This would explain the deviation from the ideal composition toward the thallium-rich side (see above) and the deviation of the europium valence toward the Eu^{3+} configuration (see below). These two chemical modifications result in an increase in the number of electrons in the valence region. In the ELF representation, the crystal structure of EuMgTl must be understood as a three-dimensional, covalently bonded polyanionic [MgTl] network in the cavities of which the europium cations are embedded.

(34) Duwell, E. J.; Baenziger, N. C. *Acta Crystallogr.* **1955**, *8*, 705.
(35) Hoffmann, R.-D.; Pöttgen, R. *Z. Kristallogr.* **2001**, *216*, 127.
(36) Iandelli, A. *Z. Anorg. Allg. Chem.* **1964**, *330*, 221.
(37) Krypyakevich, P. I.; Evdokimenko, V. I.; Zalutsky, I. I. *Dopov. Akad. Nauk Ukr. RSR* **1964**, 766.
(38) Friauf, J. B. *Phys. Rev.* **1927**, *29*, 35.
(39) Komura, Y.; Tokunaga, K. *Acta Crystallogr.* **1980**, *B36*, 1548.
(40) Emsley, J. *The Elements*; Oxford University Press: Oxford, U.K., 1999.
(41) Donohue, J. *The Structures of the Elements*; Wiley: New York, 1974.
(42) Sichevich, O.; Ramlau, R.; Giedigkeit, R.; Schmidt, M.; Niewa, R.; Grin, Y. Presented at the 13th International Conference on Solid Compounds of Transition Elements, Stresa, Italy, 2000; p O-13.
(43) Kohout, M.; Wagner, F. R.; Grin, Y. *Theor. Chem. Acc.* **2002**, *108*, 150.

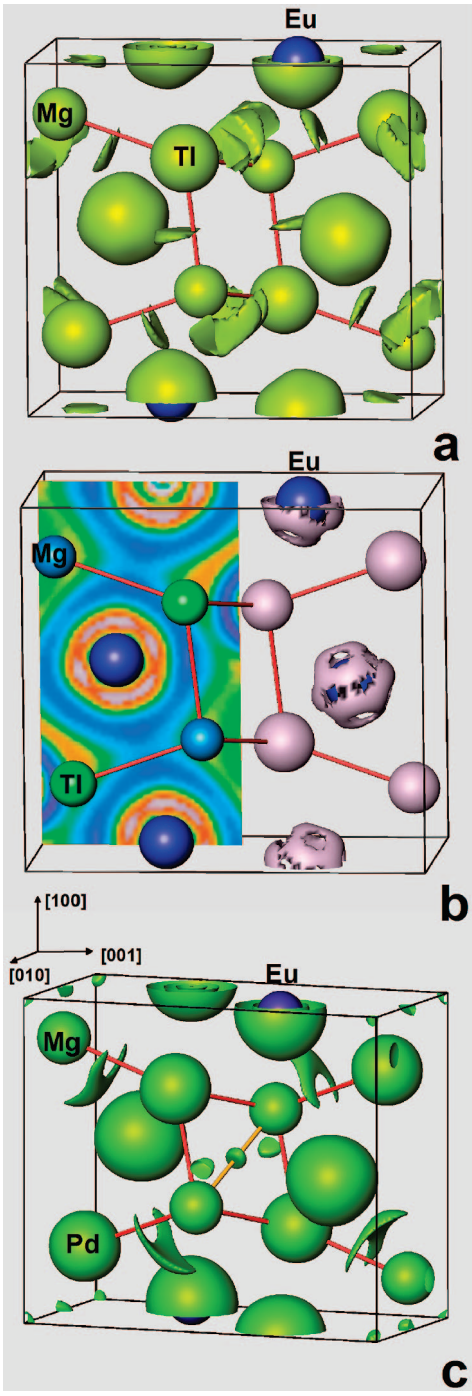

Figure 4. Electron localization function in (a, b) EuMgTl and (c) EuMgPd.

The topology of the ELF in the region of the polyanion in the isotypic compound EuMgPd (Figure 4c) is similar to that in EuMgTl. Each of the Mg−Pd contacts possesses its own ELF maximum, confirming the direct interaction within the polyanion. Additional attractors were found on the short Mg−Mg contacts in the Mg_2Pd_2 parallelogram, indicating the additional interaction that was already pointed out by the different distribution of the interatomic distances (as described above). Thus, a magnesium-containing polyanion is also formed in EuMgPd. The electron deficiency of the polyanion in this compound is greater than in EuMgTl, and the polyanion should be considered as $[MgPd]^{4-}$. An analogy to the case of EuMgTl might suggest that this problem could

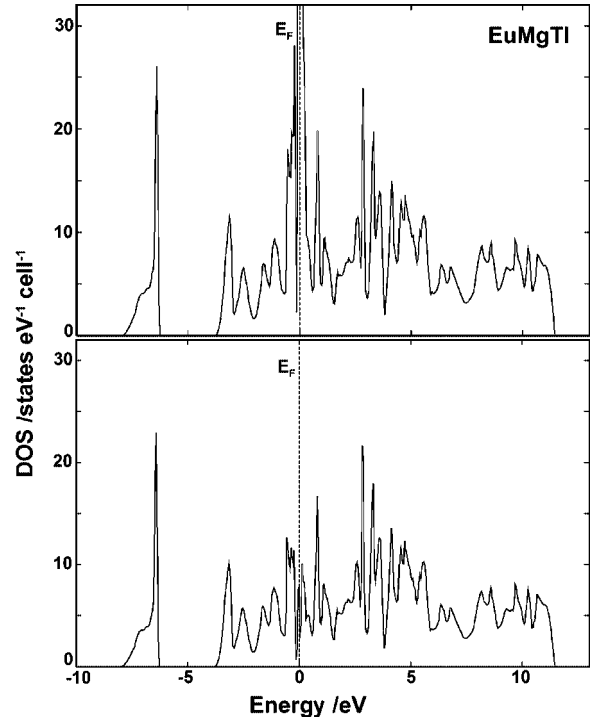

Figure 5. (top) Total electronic density of states for EuMgTl. (bottom) Partial DOS calculated without the Eu(4f) contributions, for comparison with the total DOS.

be solved through a strong palladium substitution on the Mg site. However, refinement of the occupancy parameters of the palladium and magnesium sites of EuMgPd revealed full occupancies within two estimated standard deviations.[28] Thus, the formation of the additional Mg−Mg bonds is a consequence of this electronic situation.

The picture of magnesium and thallium or palladium participating in the same polyanion is an unusual one, but it seems to be possible in intermetallic compounds. Similar situations were also observed in the chemically related gallium phases $EuMg_xGa_{4-x}$, $EuLi_xGa_{4-x}$,[44] and $EuLi_xGa_{2-x}$,[45] in the substructures of which magnesium or lithium replaces gallium but not europium.

3.2. Magnetic and Spectral Behavior. The temperature dependence of the inverse of the magnetic susceptibility of EuMgTl (measured on a sample with the 1/1/1 starting composition prepared using the Schlenk technique) is shown in Figure 6. Above 100 K, a Curie−Weiss-like behavior with an experimental magnetic moment (μ_{eff}) of 7.84(5) μ_B/Eu atom and a paramagnetic Curie temperature (θ_P) of 23(1) K was observed. The analogous measurement on a sample with the 1/1/1 starting composition prepared in a glovebox yielded $\mu_{eff} = 7.84(5)$ μ_B/Eu atom and $\theta_P = 20(1)$ K, giving a good estimate for the total error of the experiments. The experimental magnetic moment in both experiments was slightly but definitely smaller than the theoretical effective moment of 7.94 μ_B/Eu atom for the free Eu^{2+} ion.[46] Use of the latter value for comparison yields an estimated effective europium

(44) Fedorchuk, A. O.; Prots, Y.; Grin, Y. *Z. Kristallogr.—New Cryst. Struct.* **2005**, *220*, 317.
(45) Fedorchuk, A. O.; Prots, Y.; Schnelle, W.; Grin, Y. *Z. Kristallogr.—New Cryst. Struct.* **2005**, *220*, 315.
(46) Lueken, H. *Magnetochemie*; Teubner: Stuttgart, Germany, 1999.

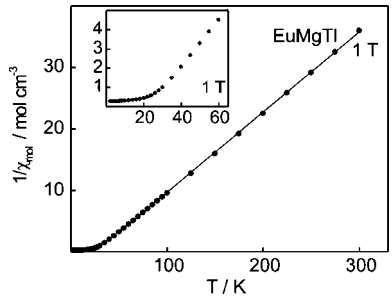

Figure 6. Temperature dependence of the inverse of the magnetic susceptibility of EuMgTl measured at a flux density of 1 T. The low-temperature behavior is shown in the inset.

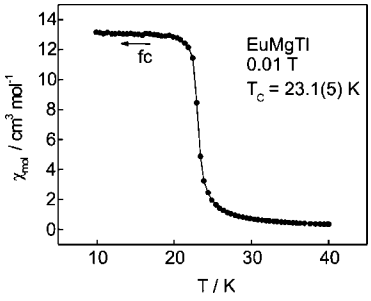

Figure 7. Low-temperature magnetic susceptibility of EuMgTl measured at a flux density of 0.01 T in field-cooling (fc) mode. The Curie temperature of 23.1(5) K was determined from the derivative dχ/dT.

configuration of $Eu^{2.03+}$, which is very close to Eu^{2+} but has a charge smaller than that obtained from spectroscopic measurements (see below). Because of the polarization of the conducting electrons, the effective paramagnetic moment for europium in the compound may be enhanced compared with the value for the free ion. The values of 7.78 and 8.52 μ_B/Eu atom were observed for the binary compounds $EuTl_2$[36] and $EuMg_2$,[47] respectively. Taking the average of these results (8.15 μ_B/Eu atom) as a reference, one obtains the effective configuration $Eu^{2.08+}$, which is in agreement with the XAS and Mössbauer measurements described below.

The magnetic data gave no hint of surface oxidation. In the latter case, one first observes formation of EuO, which orders ferromagnetically at 70 K.[1] No bump was observed in the plot of $1/\chi$ versus T for any of the EuMgTl samples.

The sharp increase in magnetic susceptibility at 23 K indicated ferromagnetic ordering of the europium magnetic moments. The magnetic behavior at low temperature (i.e., field-cooling data) in an external field of only 0.01 T is presented in Figure 7. The Curie temperatures of 23.1(5) and 23.4(4) K (for the samples prepared using the Schlenk technique and the glovebox, respectively) were determined from the derivatives dχ/dT. The field dependence of the magnetization is shown in Figure 8. At room temperature, linear behavior of $M(B)$ was observed, as expected for a paramagnetic material. The magnetization at the highest obtainable field (9 T) was only 0.45 μ_B/Eu atom. At 10 K, the magnetization steeply increased and almost reached saturation at 9 T. The magnetic moment of 6.90 μ_B/Eu atom was slightly smaller than the theoretical moment of 7 μ_B found from $g \times S$.[46]

(47) Buschow, K. H. J.; Sherwood, R. C.; Hsu, F. S. L.; Knorr, K. *J. Appl. Phys.* **1978**, *49*, 1510.

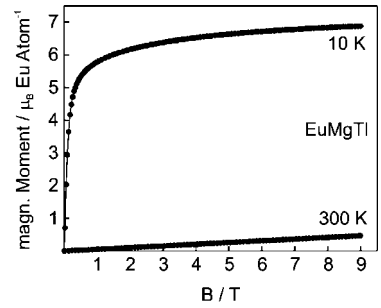

Figure 8. Magnetization of EuMgTl as a function of external magnetic field strength measured at 10 and 300 K.

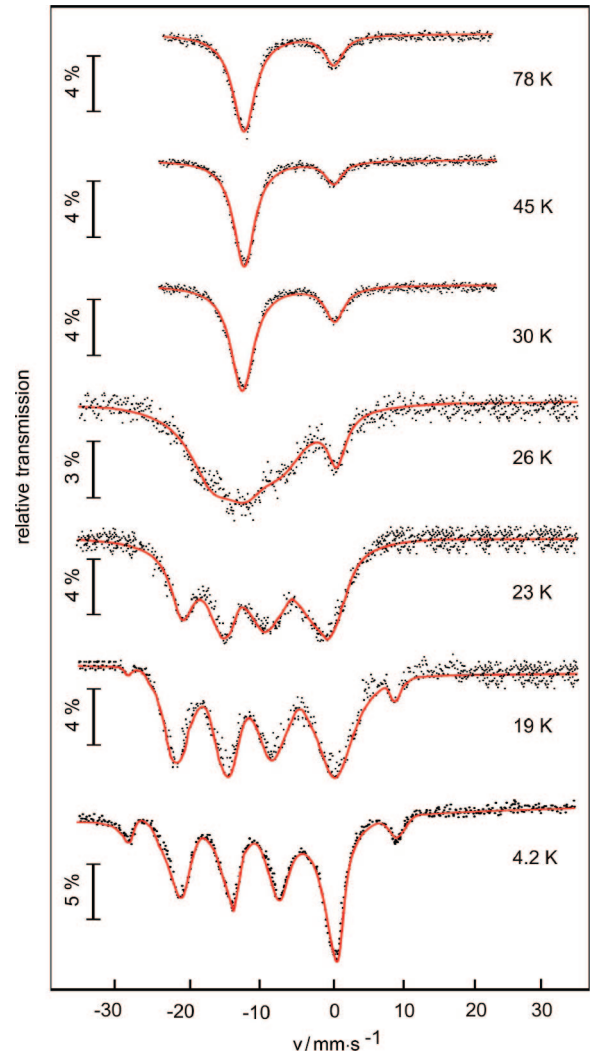

Figure 9. Experimental and simulated ^{151}Eu Mössbauer spectra of EuMgTl at various temperatures.

^{151}Eu Mössbauer spectra of EuMgTl at various temperatures together with transmission-integral fits are presented in Figure 9. The corresponding fitting parameters are listed in Table 6. The spectra show signals near −10 and 0.6 mm/s, indicating the presence of Eu^{2+} and Eu^{3+}, respectively, in EuMgTl. The Eu^{2+} signal was subjected to a small amount of quadrupole splitting. The experimentally observed line widths were nearly equal to the natural line width of ^{151}Eu.

At 78 K, an isomeric shift value (δ) of −10.1 mm/s for the Eu^{2+} signal was observed. In a recent paper, the isomeric shifts for the whole series of EuTX intermetallic compounds

Table 6. Fitting Parameters for ^{151}Eu Mössbauer Measurements on EuMgTl: Isomeric Shift (δ), Electric Quadrupole Splitting (ΔE_Q), Magnetic Hyperfine Field ($|B_{hf}|$), and Experimental Line Width (Γ)[a]

temperature (K)	δ_1 (mm/s)	ΔE_{Q1} (mm/s)	$\lvert B_{hf}\rvert$ (T)	Γ_1 (mm/s)	δ_2 (mm/s)	Γ_2 (mm/s)	Eu^{2+}/Eu^{3+}
78	−10.14(1)	0.33(8)	−	1.93(1)	0.62(5)	2.83(1)	86/14
45	−10.06(6)	0.28(5)	−	2.18(4)	0.64(2)	2.79(2)	85/15
30	−10.11(7)	0.33(3)	−	2.29(7)	0.67(5)	2.75(1)	83/17
26	−10.10(3)	−0.15(1)	8.6(4)	6.41(3)	0.59(5)	2.20(3)	82/18
23	−10.10(2)	−0.15(7)	17.6(1)	3.24(1)	0.63(4)	2.48(2)	82/18
19	−10.04(1)	−0.16(1)	19.9(3)	2.91(9)	0.66(1)	3.08(1)	80/20
4.2	−10.11(5)	−0.16(2)	23.4(4)	2.40(2)	0.71(2)	2.98(2)	76/26

[a] Numbers in parentheses represent the statistical errors in the last digit. Subscripts 1 and 2 refer to the Eu^{2+} and Eu^{3+} signals, respectively.

were correlated with the valence electron count (VEC, equal to the number of valence electrons plus 10).[48] For EuMgTl, which has 7 valence electrons per formula unit, the isomer shift fits well at VEC = 17 in the plot of δ versus VEC, as expected.

The onset of magnetic ordering was detected at 26 K. Slightly below the ordering temperature, the static magnetic flux density at the europium nuclei was small, and the uncertainty was also expressed in the higher values of line width parameter (Γ_1) at 26 and 23 K. Most likely this increased uncertainty resulted from the fact that europium species in different environments arising from Mg/Tl substitution within the polyanion have slightly different ordering temperatures. The flux density then increased with decreasing temperature. Full magnetic hyperfine field splitting was observed at 4.2 K with a static magnetic flux density of 23.4 T, as frequently observed in related Eu*TX* compounds.[1] The Eu^{2+}/Eu^{3+} ratio was almost constant over the whole temperature range (14% of Eu^{3+}, corresponding to an effective configuration of $Eu^{2.14+}$; see the XAS data below). Only at very low temperatures, well below the Curie temperature, was a slight increase in the Eu^{3+} percentage observed (Table 6). At this point it is important to note that this Eu^{2+}/Eu^{3+} ratio was observed for four samples prepared with different techniques.

The onset of magnetic ordering was associated with a change in the magnitude of the electric field gradient (EFG) parameter used to optimize the least-squares fit to the data. This behavior is similar to that seen in EuPdIn,[49] EuAgMg,[6] and $Eu_2Si_5N_8$[50] and most likely occurs because the angle defining the EFG principal axis is close to the magic angle.

The X-ray absorption spectrum of EuMgTl (Figure 10) was characterized by the main signal at ~6978 eV. This value is ~10 eV smaller than that observed for the EuF_3 standard [electronic configuration of $Eu^{3+}(4f^6)$] and is characteristic of the $4f^7$ electronic configuration of Eu^{2+}. In addition, a clear shoulder was observed in the EuMgTl spectrum on the high-energy side at the position of the EuF_3 standard (~6988 eV), indicating that europium was also present in the $4f^6$ configuration and resulting in an effective configuration of $Eu^{2.2+}$ (see the magnetization measurements).

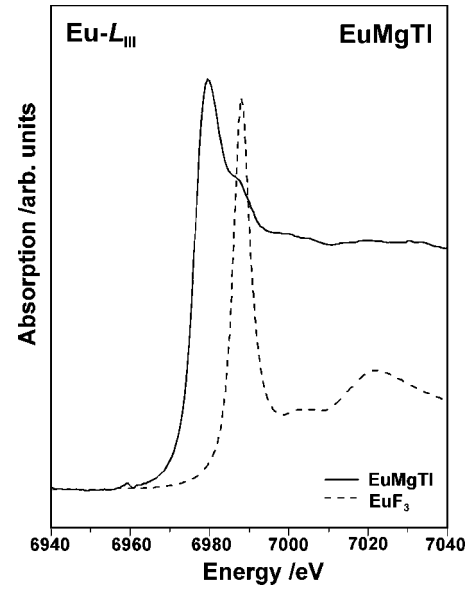

Figure 10. X-ray absorption spectra of EuMgTl (solid line) and EuF_3 as a standard for the $Eu^{3+}(4f^6)$ configuration (dashed line).

4. Conclusions

The new ternary phase $EuMg_{1-x}Tl_{1+x}$ crystallizes in the TiNiSi structure type. Bonding analysis using the electron localization function/electron density approach described the crystal structure as a three-dimensional, covalently bonded framework polyanion [MgTl] within whose cavities the europium cations are embedded. The frameworks of quadruply bonded atoms are expected to have four valence electrons per atom. $EuMg_{1-x}Tl_{1+x}$ attempts to achieve this through partial replacement of magnesium by thallium and partial oxidation of europium to the Eu^{3+} state, whereby the fully electron-balanced situation is not realized. The tendency for europium to transfer more than two electrons to the polyanion was revealed by the results of X-ray absorption and Mössbauer spectroscopy and magnetic susceptibility measurements and is in agreement with the chemical bonding analysis.

Acknowledgment. We acknowledge the valuable support of Dr. M. Baitinger during the preparative work, and we thank H.-J. Göcke for the work done at the scanning electron microscope and B. Heying and Dipl.-Ing. U. Ch. Rodewald for collection of the diffractometer data. Financial support by the Deutsche Forschungsgemeinschaft is gratefully acknowledged. C.P.S. is indebted to the NRW Graduate School of Chemistry for a Ph.D. stipend.

CM071325I

(48) Müllmann, R.; Ernet, U.; Mosel, B. D.; Eckert, H.; Kremer, R. K.; Hoffmann, R.-D.; Pöttgen, R. *J. Mater. Chem.* **2001**, *11*, 1133.
(49) Müllmann, R.; Mosel, B. D.; Eckert, H.; Kotzyba, G.; Pöttgen, R. *J. Solid State Chem.* **1998**, *137*, 174.
(50) Höppe, H. A.; Trill, H.; Mosel, B. D.; Eckert, H.; Kotzyba, G.; Pöttgen, R.; Schnick, W. *J. Phys. Chem. Solids* **2002**, *63*, 853.